Sensor and Simulation Notes

Note 570

Idus Martiae 2015

Design of a Certain Class of Broad Band Dipole Antennas

I L Gallon
41, St Katherine's Avenue, Bridport, Dorset, DT6 3DE, UK
E-mail: ilandpamgallon@tiscali.co.uk

and

D V Giri
Pro-Tech, 11-C Orchard Court, Alamo, CA 94507, USA
Dept. of E. C. E., University of New Mexico, Albuquerque, NM, USA

Abstract

Antennas are regarded as transmission lines with space dependent parameters. The frequency response is generally scale dependent. However, imposing frequency independence on the transmission line equations leads to a scale independent geometry.

1. Introduction

Bandwidth can be an important attribute of an antenna, if it is required to perform over a range of frequencies. Other performance parameters of any antenna can be summarized by an acronym BRIDGE [1] denoting **B**eamwidth, **R**adiation pattern, **I**nput impedance, **D**irectivity, **G**ain and **E**ffective area. In this note, we focus on the bandwidth and investigate a way of improving the bandwidth. When we talk of the bandwidth of an antenna, we need to distinguish between two types which we will call i) CW bandwidth and ii) transient bandwidth. For instance, when the so called "Frequency Independent Antennas" came on the scene in 1958 [2], it is noted that this class of antennas have a large CW bandwidth. A log periodic antenna works for a large range of frequencies, if these frequency signals are applied at different times. It is highly dispersive and does not work if one applies a transient pulse which contains many frequencies at the same time. In other words, a log-periodic antenna has a large CW bandwidth and no transient bandwidth to speak of. If we apply a pulse to a log periodic antenna , different frequency components get radiated from different parts of the antenna and reach an observer at a distance at slightly different times resulting in a significant loss of pulse fidelity. Essentially the phase centre of the log periodic antenna is not stationary. Pulsed antennas have received a lot of attention in recent years and a good example is the Impulse Radiating Antenna [3-5]. Such an antenna is TEM wave-fed and hence non-dispersive. It has a large transient bandwidth and can also be used at single CW frequency over a wide (100 to 1) frequency band.

There exist a number of methods for increasing the bandwidth of antennas. Increasing the diameter of the elements of a dipole [6], assembling arrays of non-resonant antennas [7], specifying the antenna shape by angles [2], varying the impedance with position so as to inhibit reflections [8]. The first three approaches have relatively severe limitations, approach 1 only producing a modest range, approach 2 results in a frequency dependent direction, and approach 3 requires an infinite scale. It is the last approach that is developed here. It is found that finite structures exist that support outgoing waves with no reflections.

2. The Approach

An antenna is modelled as a transmission line with position dependent parameters, and a wave solution is sought that maintains the wave shape as it progresses.

The transmission line (TL) equations are

$$\frac{\partial V}{\partial x} = -L' \frac{\partial I}{\partial t} \tag{1}$$

$$\frac{\partial I}{\partial x} = -C' \frac{\partial V}{\partial t} \tag{2}$$

where L' and C' are the inductance and capacitance per unit length of line.

Letting the inductance be a function of position

$$L' = L'(x) \tag{3}$$

Eliminating the current I from the TL equations, we obtain

$$\frac{\partial^2 V}{\partial x^2} = \frac{1}{L'} \frac{\partial L'}{\partial x} \frac{\partial V}{\partial x} + L'C' \frac{\partial^2 V}{\partial t^2} \tag{4}$$

noting that

$$L'C' = \frac{1}{c^2} \tag{5}$$

for a line with dielectric ε_0. We now look for a solution representing an arbitrary travelling voltage wave with varying amplitude

$$V = V_0(x)f(x - ct) \tag{6}$$

Inserting this function into the differential equation

$$\left\{\frac{d^2V_0}{dx^2} - \frac{1}{L'}\frac{dL}{dx}\frac{V_0}{x}\right\} f(x-ct) + \left\{2\frac{dV_0}{dx} - \frac{1}{L'}\frac{dL'}{dx}\right\} f'(x-ct) = 0 \tag{7}$$

V_0 is independent of t and so we must have

$$\left\{\frac{d^2V_0}{dx^2} - \frac{1}{L'}\frac{dL'}{dx}\frac{dV_0}{dx}\right\} = 0 \tag{8}$$

$$\left\{2\frac{dV_0}{dx} - \frac{1}{L'}\frac{dL'}{dx}V_0\right\} = 0 \tag{9}$$

An arbitrary choice of the inductance variation will not in general be compatible with both the above equations. Eliminating V_0 there results

$$\frac{1}{2}\left(\frac{1}{L'}\frac{dL'}{dx}\right)^2 = \frac{d}{dx}\left(\frac{1}{L'}\frac{dL'}{dx}\right) \tag{10}$$

The solution of this equation, for a line of length ℓ is

$$L' = L_0' \frac{1}{\left(1 - \frac{x}{\ell}\right)^2} \tag{11}$$

Substituting this result into the first order equation for V_0 and integrating

$$V_0 = V_{00}\frac{1}{1 - \frac{x}{\ell}} \tag{12}$$

We must have

$$L_0' \frac{C'}{\left(1 - \frac{x}{\ell}\right)^2} = \frac{1}{c^2} \tag{13}$$

or

$$C' = \frac{\left(1 - \frac{x}{\ell}\right)^2}{c^2 L_0'} = C_0'\left(1 - \frac{x}{\ell}\right)^2 \tag{14}$$

With this variation of parameters with position we have a frequency independent transformer where the impedance is, for a length X,

$$Z_{out} = \sqrt{\frac{L'}{C'}} = \sqrt{\frac{L_0'}{C_0'}} \frac{1}{\left(1-\frac{X}{\ell}\right)^2} = Z_{in} \frac{1}{\left(1-\frac{X}{\ell}\right)^2} \tag{15}$$

If the transformer is left open circuit, we have an antenna. Not only is it frequency independent, it is also scale independent. Practically there will be limitations; in particular we cannot expect the highest frequency to be greater than that indicated by the dimensions of the feed. The low frequency limit is more difficult to define. Matching the antenna to Z_0 for a $50\,\Omega$ input impedance

$$\frac{X}{\ell} = 1 - \sqrt{\frac{50}{376.73}} = 0.6357 \tag{16}$$

The dependence of the impedance on the ratio of the dimensions means that the set of antenna designs is infinite. A few of the more interesting designs are considered below.

3. TEM Horn Antennas

A TEM horn antenna can be considered first as a triangular plate transmission line

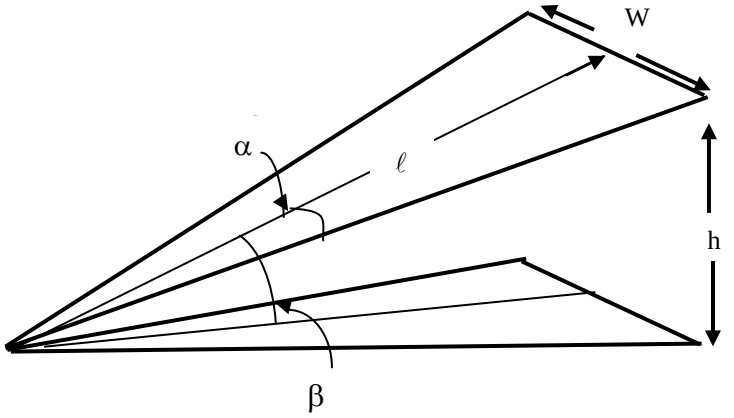

Figure 1. A TEM horn antenna viewed as a triangular plate transmission line

The impedance of this line is given approximately by

$$Z = Z_0 \frac{h}{W} \tag{17}$$

where Z_0 is the impedance of free space. As the impedance depends only on angle it is independent of frequency, provided the plates extend to infinity. If we now express W as a function of x measured along the mid plane,

$$W = 2x \frac{\tan\left(\frac{\alpha}{2}\right)}{\cos\left(\frac{\beta}{2}\right)} \tag{18}$$

and put

$$h = 2x \tan\left(\frac{\beta}{2}\right) \tag{19}$$

We then have

$$Z = Z_0 \frac{\tan\left(\frac{\beta}{2}\right)\cos\left(\frac{\beta}{2}\right)}{\tan\left(\frac{\alpha}{2}\right)} = \frac{Z_0 \sin\left(\frac{\beta}{2}\right)}{2\tan\left(\frac{\alpha}{2}\right)} \tag{20}$$

Reflections from the ends of finite planes limit the bandwidth. It is to be expected that for ($\beta < \pi$) there will be some enhanced directionality to the radiated field, but this has not been investigated. Assuming a moderate amount of directionality is of benefit, we choose $\beta = \pi/2$. Then, taking the initial impedance as 50Ω

$$\tan\frac{\alpha}{2} = \frac{377}{2 \times 50 \times \sqrt{2}} = 2.67 \tag{21}$$

giving

$$\alpha = 138.9^o \tag{22}$$

We then impose the width variation, leading to a finite line

$$\frac{W}{2} = x \tan\left(\frac{\alpha}{2}\right)\left(1 - \frac{x}{\ell}\right)^2 = 2.67\, x\left(1 - \frac{x}{\ell}\right)^2 \tag{23}$$

There is a significant error, of order 10%, in the approximation due to ignoring the fringe fields. The approximation may be improved, and is investigated later. Note that the antenna length can be reduced by taking it such that the end impedance has some high some high value, 377Ω being an obvious choice. Note that this has the wrong dimensions to match free space! The need to so modify designs is the requirement for excessively large or small dimensions.

Setting $Z=Z_0$ we require

$$\frac{\sin\left(\frac{\beta}{2}\right)}{\tan\left(\frac{\alpha}{2}\right)}\left(1 - \frac{x}{\ell}\right)^{-2} = 1 \tag{24}$$

leading to

$$\frac{x}{\ell} = 1 - \sqrt{\frac{\sin(\beta/2)}{\tan\frac{\alpha}{2}}} \tag{25}$$

For 50Ω and 100Ω and $\beta=\pi/2$, $\frac{X}{\ell} = 0.485$, 0.636.

3.1 Fringe Field Correction

An approximation for the fringe field of a parallel plate transmission line due to Palmer [9] is

$$C' = \varepsilon_o \frac{W}{h}\left\{1 + \frac{h}{\pi W}\left(1 + \ln\left[\frac{2\pi W}{h}\right]\right)\right\} \tag{26}$$

Palmer compares the above approximation with the "exact" solution from the Schwartz-Christoffel transformation for values of (W/h) in the limited range from 0 to 2. The approximation in equation (26) is reasonable for 0.5 < (W/h) < 2. Unfortunately, as the width approaches zero the formula diverges. Including a function of W/h that varies from zero to one in the argument of the logarithmic term removes the divergence and has little effect away from zero, where [10] shows the approximation is accurate. We then have

$$C' = \varepsilon_0 \frac{W}{h}\left\{1 + \frac{h}{\pi W}\left(1 + \ln\left[f\left(\frac{W}{h}\right) + \frac{2\pi W}{h}\right]\right)\right\} \tag{27}$$

Similarly

$$L' = \mu_o\left[\frac{W}{h}\left\{1 + \frac{h}{\pi W}\left(1 + \ln\left[f\left(\frac{W}{h}\right) + \frac{2\pi W}{h}\right]\right)\right\}\right]^{-1} \tag{28}$$

There is a further correction term for thick plates due to Yang [11] that has been ignored. The expression for the impedance then becomes

$$Z = Z_o \frac{h}{W}\left\{1 + \frac{h}{\pi W}\left(1 + \ln\left[f\left(\frac{W}{h}\right) + \frac{2\pi W}{h}\right]\right)\right\}^{-1} \tag{29}$$

We then require

$$Z = Z_o \frac{h}{W}(0)\left\{1 + \frac{1}{\pi}\frac{h}{W}(0)\left(1 + \ln\left[2\pi\frac{W}{h}(0)\right]\right)\right\}^{-1}\left\{1 - \frac{x}{\ell}\right\}^{-2} \tag{30}$$

$$\frac{h(x)}{W(x)}\left\{1 + \frac{1}{\pi}\frac{h(x)}{W(x)}\left(1 + \ln\left[f\left(\frac{W}{h}\right) + 2\pi\frac{W(x)}{h(x)}\right]\right)\right\}^{-1} = \frac{h}{W}(0)\left\{1 + \frac{1}{\pi}\frac{h}{W}(0)\left(1 + \ln\left[2\pi\frac{W}{h}(0)\right]\right)\right\}^{-1}\left\{1 - \frac{x}{\ell}\right\}^{-2} \tag{31}$$

Setting

$$u = \frac{W(x)}{h(x)} = \frac{W(x)}{2x\tan\frac{\beta}{2}} \quad \text{and} \qquad f = \exp\{-\kappa u\} \tag{32}$$

where κ is some suitable number,

$$\frac{1}{u}\left\{1+\frac{1}{\pi u}\left(1+\ln\left[\exp\left(-\kappa u\right)+2\pi u\right]\right)\right\}^{-1}=A^{-1}\left\{1-\frac{x}{\ell}\right\}^{-2} \tag{33}$$

We then have

$$\frac{x}{\ell}=1-\sqrt{\frac{1}{A}\left\{u+\frac{1}{\pi}\left(1+\ln\left[\exp\left(-\kappa u\right)+2\pi u\right]\right)\right\}} \tag{34}$$

where A is given by

$$A=\frac{W}{h}(0)+\frac{1}{\pi}\left[1+\ln\left\{2\pi\frac{W}{h}(0)\right\}\right]=\frac{Z_0}{Z(0)} \tag{35}$$

For $\beta=\frac{\pi}{2}$ and Z(0) = 50 and 100 Ω ,

$$A=\frac{377}{50}=7.54 \text{ and } \frac{377}{100}=3.77 \tag{36}$$

A graphical solution shown in figure 2, then gives

$\frac{W}{h}(0)=6.061$ *and* 2.567 respectively and κ=2. It was found that the curves changed very slowly over equation (56) over the range of 0.1-5 for κ. From the definition of u we have

$$\frac{W(x)}{2\ell}=\frac{x}{\ell}u\ \tan\left(\beta/2\right) \tag{37}$$

For $\beta=\pi/2$

$$\frac{W(x)}{2}=xu \tag{38}$$

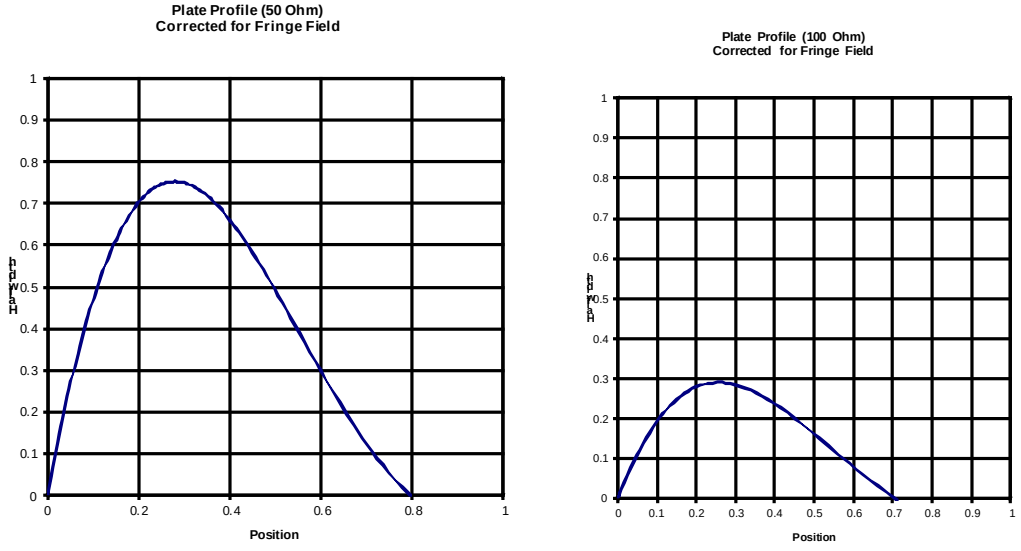

(a) 50 Ohm case (x/ℓ) (b) 100 Ohm case (x/ℓ)

Figure 2. Plate profile with fringe field correction

Comparing the corrected with the uncorrected profiles the half width maximum is in error by ~7% for the 50Ω line and ~33% for the 100Ω line, while the length is in error by~ 25% and ~ 40% respectively. This error is discussed later.

At this point, it is relevant to review some related published work in the literature on this topic.

Numerical evaluation of the characteristic impedance of a TEM horn of finite length has been extensively calculated and tabulated [12], using the method of stereographic transformation. Conformal transformation techniques are available for two-dimensional problems, and a stereographic projection is needed for a three-dimensional problem. A TEM horn has a spherical wave front which is three-dimensional.

One approach uses the method of terminating the TEM horn in its characteristic impedance to avoid reflections [13-15]. There are several ways to terminate a TEM horn. Figure 3 illustrates some examples of back-termination of the TEM horns. Such a back termination minimizes the back radiation at low frequencies. At low frequencies, (wavelengths large compared to horn dimensions), the TEM horn is characterized by a pair of electric ($\vec{p}$) and magnetic dipole ($\vec{m}$). The resultant radiation is in the direction ($\vec{p}x\vec{m}$) which is orthogonal to both dipole moments. If the TEM horn is terminated at the exit aperture, the resultant radiation at low-frequencies is in the backward direction. Back termination reverses the direction of the magnetic dipole moment and results in the low-frequencies going out in the bore sight direction.

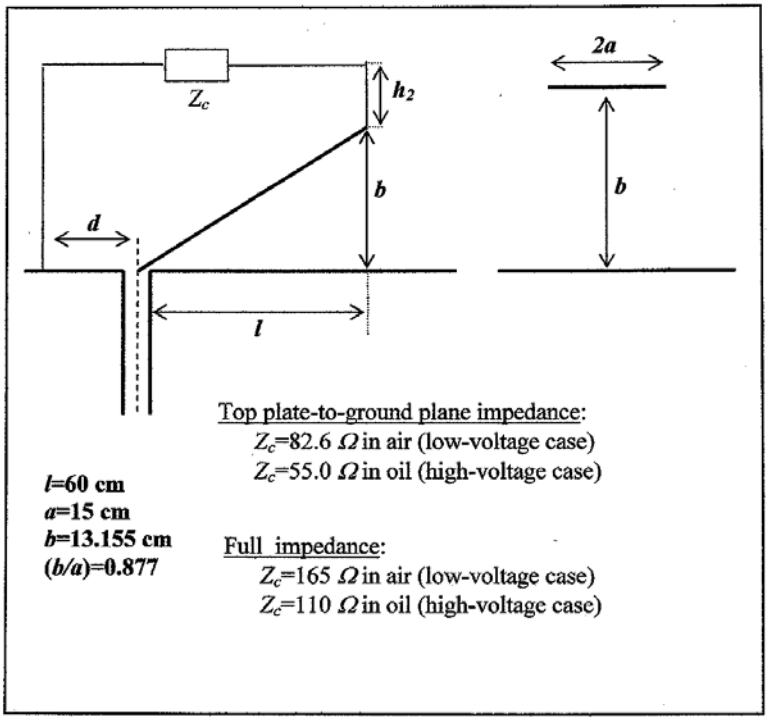

Figure 3. Back- terminated TEM horn [reproduced here from [15]

Bandwidth of a TEM horn is enhanced by both lowering the low frequency cut off and increasing the high-frequency cutoff.

It is also recalled that a TEM horn, unlike a dipole antenna is an aperture type of antenna. This means the radiated field from the aperture of a TEM horn is a time derivative of the aperture field. This was experimentally demonstrated in [16] where they considered a TEM horn as a transmission line and attempted, without much success, to apply the integral of a double exponential pulse at the input in order to radiate a double exponential pulse.

The second is an experimental approach [17] along the lines suggested in this note, by controlling the impedance as a function of position. In [17], they use a FDTD numerical method to analyze three different types of TEM horns.

1) A constant impedance TEM horn with no change of impedance as a function of position
2) A shaped TEM horn with a resistive termination at the open end
3) A TEM horn where the plates have a resistance varying continuously along its length

In all three cases (shown in Figure 4) the reflected voltage from the open end is estimated and measured. It is clear that this reflection degrades the performance of the antenna in terms of bandwidth and radiated waveform features. At the apex of the horn, the characteristic impedance is set equal to that of the feeding line, typically 50 Ohms. One can then set the impedance at the aperture to be 377 Ohms like we considered before. The idea is that there would be very little reflection from the open end if the impedance of the line is 377 Ohms at the end. In fact, they find this to be not the case. This has been called the TWIT (travelling wave, impedance taper) TEM horn. The impedance as a function of position is varied in a special manner. Resistive cards were placed over the plates at the very end to further reduce the reflections. The excitation voltage was a Gaussian voltage pulse and the reflected voltage is measured in the feed coax. The peak of reflected voltage (in time domain) from the open end was measured to be about 41% of the incident voltage. So, arranging for 377 Ohm impedance at the open end appears to be an erroneous concept, probably because 377 Ohms is the impedance of a uniform plane wave in free space and that is not what we have at the open end of a TEM horn. Shlager et al [17] also found that the reflections reduced from 41% to 27%, if they introduced resistive sheets at the end in addition to the matching to 377 Ohms. Example of the TEM horn where it is continuously loaded by a triangular resistive profile

$$r(x) = \frac{r(0)}{1-(x/\ell)} \quad , \quad 0 < x < \ell \tag{39}$$

Is in accordance with Wu-King profile described in [18] in the context of a cylindrical dipole antenna. Here *r(0)* is the resistance per unit length at the apex and it gradually increases to near infinity (or very large values) at the open end. Here the idea is that the current flowing on the plate essentially decays out so that there is nothing to reflect back, thus eliminating the resonance of the horn plates.

In conclusion one might say that proper loading can improve the bandwidth of the TEM horn and there are techniques available to lower the low-frequency cutoff and increase the high-frequency cut off. However, there is no escaping the fact that the radiated field of an aperture antenna such as the TEM horn is a time derivative of the aperture field. The feed point considerations are also critical. Application of high voltages at the feed requires space to avoid breakdown at the feed, which fights the high frequency cut off. Larger electrode spacing near the feed necessarily lowers the high-frequency performance of the antenna. This is the perennial problem of high voltages and high frequencies.

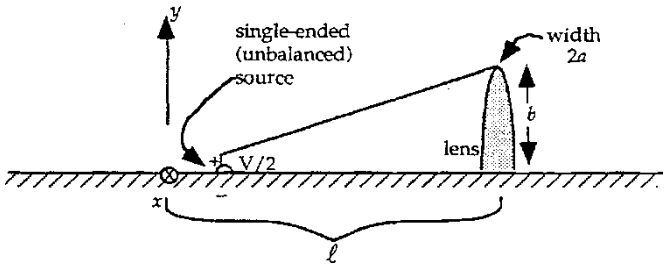

(A) Unloaded and unterminated TEM horn

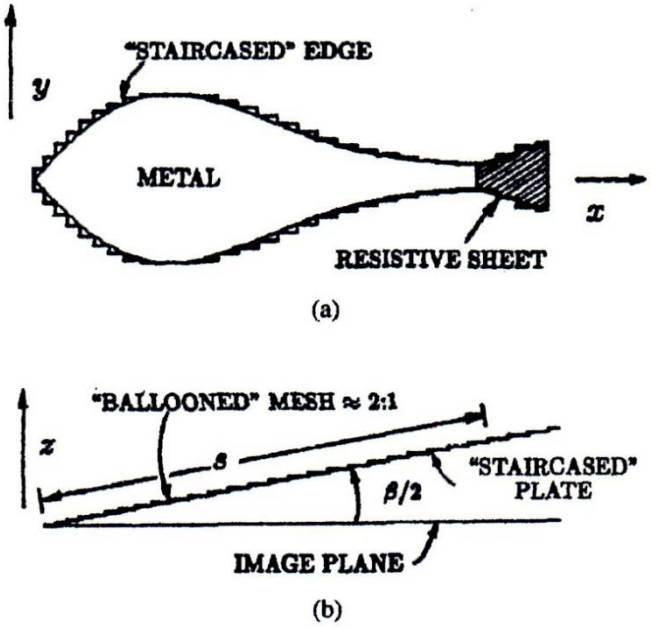

(B) Shaped and loaded to match 377Ohms/square

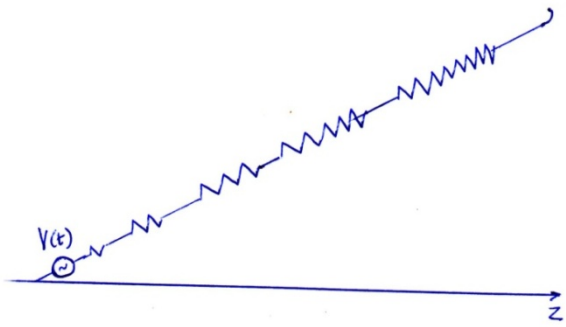

(C) Continuously loaded using Wu-King [18] loading profile

Figure 4. Three types of TEM horns considered in [17]

4. Modified Plate Antenna

A triangular plate antenna can be modified by bending the plates at a certain length into a parallel formation while at the same time modifying the shape to comply with the requirement for a frequency independent response

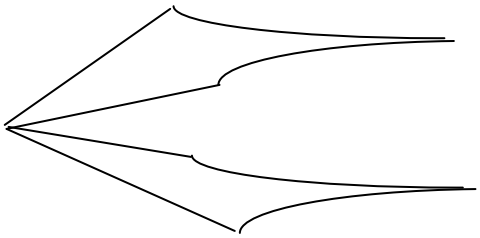

Figure 5. Notional modification of a TEM horn

Assuming that the impedance of the triangular portion of the plates is Z(0) frequency independence is imposed on the parallel section. Setting x=0 at the beginning of the parallel section, the impedance is given by

$$Z(x) = \frac{Z(0)}{\left[1 - \frac{x}{\ell}\right]^2} = Z_o \frac{h}{W(x)} \tag{40}$$

Solving for W

$$W = W(0)\left[1 - \frac{x}{\ell}\right]^2 \tag{41}$$

Half width of the parallel section is estimated and plotted in Figure 6.

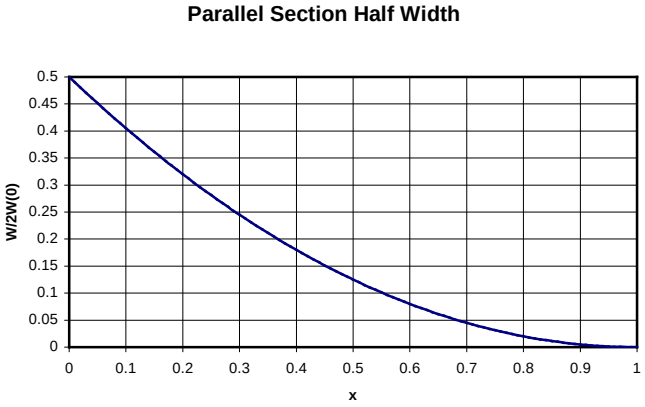

Figure 6. Calculated half width of the parallel section as a function of position

Such an antenna was fabricated and shown in Figure 7.

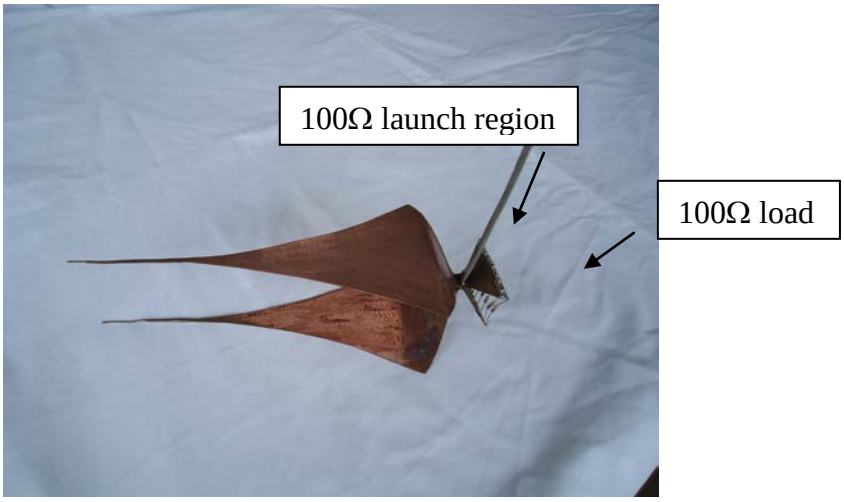

Figure 7. Photograph of a modified TEM horn antenna

Provisional measurements made with the modified TEM horn antenna of Figure 7 indicated a wide bandwidth.

One can attempt a Fringe Field Correction for the modified TEM horn antenna of Figure 5 and 7.
The impedance of the tapered section is given by

$$Z = Z_o \frac{h}{W(0)}\left\{1+\frac{1}{\pi}\frac{h}{W(0)}\left(1+\ln\left[2\pi\frac{W(0)}{h}\right]\right)\right\}^{-1}\left\{1-\frac{x}{\ell}\right\}^{-2} = Z_o \frac{h}{W(x)}\left\{1+\frac{1}{\pi}\frac{h}{W(x)}\left(1+\ln\left[2\pi\frac{W(x)}{h}\right]\right)\right\}^{-1} \quad (42)$$

Setting $u = \frac{W(x)}{h}$, we then have

$$\frac{x}{\ell} = 1 - \sqrt{\frac{u\left\{1+\frac{1}{\pi u}\left(1+\ln\left[2\pi u\right]\right)\right\}}{u(0)\left\{1+\frac{1}{\pi u(0)}\left(1+\ln\left[2\pi u(0)\right]\right)\right\}}} \quad \textbf{(43)}$$

yields W(0)/h = 6.061 for a 50Ω line and 2.567 for the 100Ω line. Calculating x as a function of u and plotting u as a function of x the following profiles of Figures 8 and 9 are obtained.

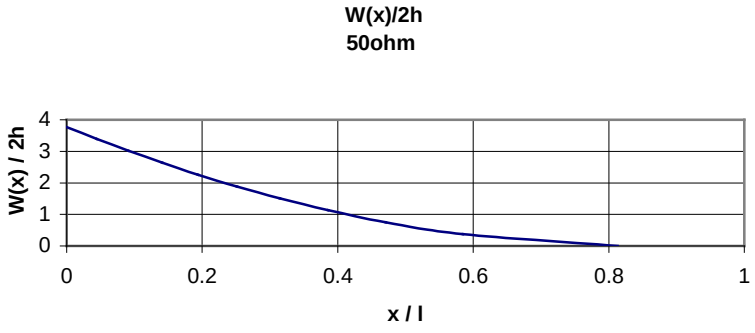

Figure 8. Profile of the width as a function of position

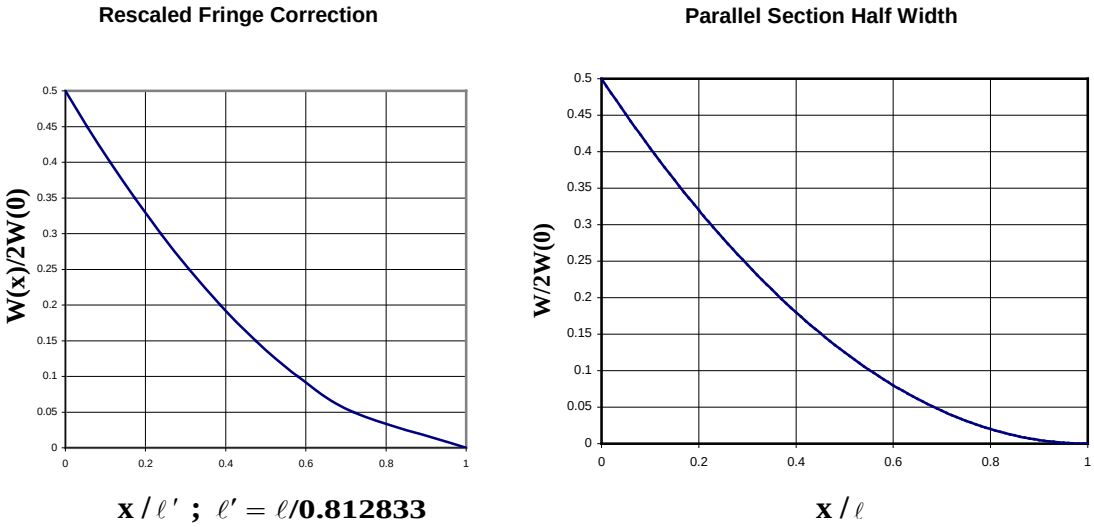

Figure 9. Rescaled width profiles as a function of position

The above comparison with the rescaled corrected profile and the uncorrected profile accounts for the broad band behaviour of the model based on the uncorrected design.

A further modification is to extend the triangular plates by a parallell pair of plates of constant width, and then to increase the separation with position. The geometry, as before, of the triangular plate is given by Figure 2. Setting β=π/2, and the impedance equal to 50Ω

$$\tan\frac{\alpha}{2} = \frac{377}{50\sqrt{2}} = 2.77 \tag{44}$$

$$\alpha = 158.8^{o} \tag{45}$$

Choosing W=0.3,

$$h = \frac{WZ}{Z_0} = \frac{0.3\times 50}{377} = 0.04m \tag{46}$$

and this determines

$$\ell = \frac{W}{2\tan\frac{\alpha}{2}} = \frac{0.3}{2\times 2.77} = 0.054m \tag{47}$$

The extension of the plates will take the form illustrated below in Figure 10. Similar considerations of shaping the plates were also addressed in [21-23].

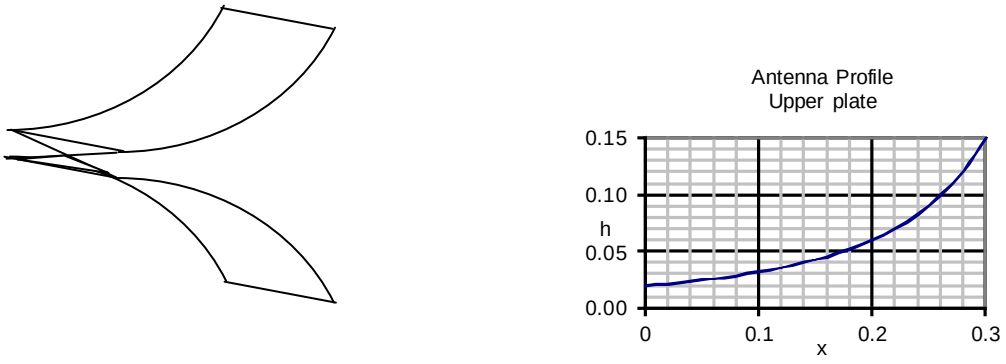

Figure 10. Flared Strip Line Antenna

The main section of the antenna is constructed as a strip line starting with a separation of h=0.04m, increasing according to

$$h = \frac{h_o}{\left(1 - \frac{x}{L}\right)^2} \tag{48}$$

where L is an arbitrary length. We can match this antenna to free space by truncating at X where $Z=Z_o$. We then have

$$\frac{X}{L} = 0.636 \tag{49}$$

We are free to choose X, and so to maintain a compact antenna, choose X=0.3m, and we have

$$L = 0.3 / 0.636 = 0.472\,\text{m} \tag{50}$$

5. The Coaxial Frequency Independent Antenna

The impedance of a coaxial line is

$$Z = \frac{Z_o}{2\pi} \ln\left\{\frac{b}{a}\right\} \tag{51}$$

Imposing frequency independence we make b dependent on position and set

$$Z(x) = \frac{Z_o}{2\pi} \ln\left\{\frac{bh(x)}{a}\right\} = Z(0)\left[1 - \frac{x}{\ell}\right]^{-2} \tag{52}$$

where $h(0) = 1$. Solving for $h(x)$

$$h(x) = \frac{a}{b}\exp\left\{\ln\left[\frac{b}{a}\right]\left[1-\frac{x}{\ell}\right]^{-2}\right\} = \left[\frac{b}{a}\right]^{\left\{\left(1-\frac{x}{\ell}\right)^2-1\right\}} \tag{53}$$

Alternatively we can make the inner radius variable. We then have, with $h(0)=1$

$$\frac{1}{g(x)} = \exp\left\{\ln\left[\frac{b}{a}\right]\left[1-\frac{x}{\ell}\right]^{-2}\right\} = \left[\frac{b}{a}\right]^{\left\{\left(1-\frac{x}{\ell}\right)^2-1\right\}} \tag{54}$$

yielding

$$h(x)\ g(x) = 1 \tag{55}$$

The ratio b/a is 2.301 for 50Ω and 5.294 for 100Ω. The electrode profiles are shown plotted in Figure 11.

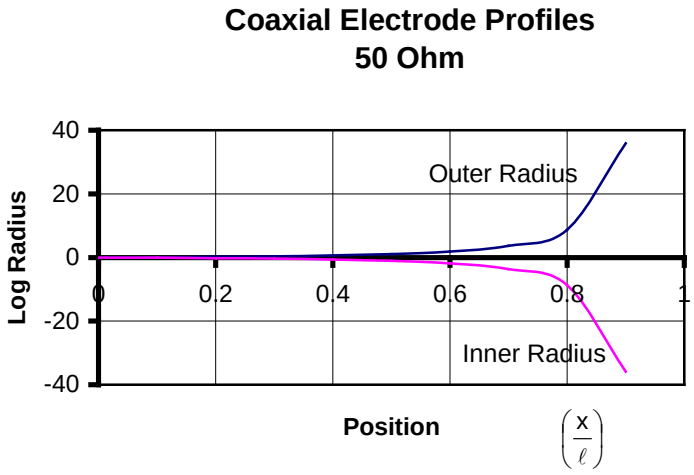

Figure 11. Electrode profiles of a coaxial transmission line antenna

Only varying the outer electrode rapidly leads to an inconveniently large radius, while only varying the inner leads to an impossibly small radius. Truncating the antenna such that the end impedance is Z_0 sets x/ℓ = 0.636, resulting in an outer radius of ~234 × Initial Radius. With an inner radius of 1mm the maximum outer radius becomes 234 × 2.301=538.4 mm, nominally seen in Figure 12.

The dimensions can be made more practical by allowing both radii to become x-dependent. For example, we may take

$$h(x) = \left(1+\alpha\frac{x}{\ell}\right) \tag{56}$$

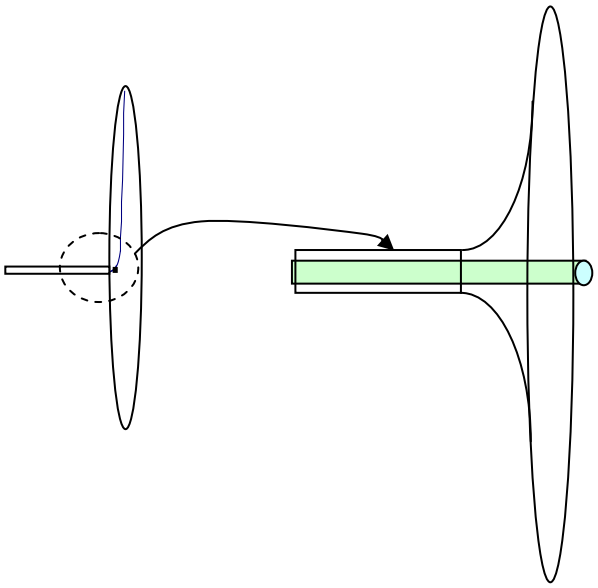

Figure 12. Coaxial Antenna terminated at 377 Ohm

where α has yet to be chosen. In Figure 13 below $\alpha = \frac{0.24}{0.07}$ =3.429 giving the angle as ~74^{o}

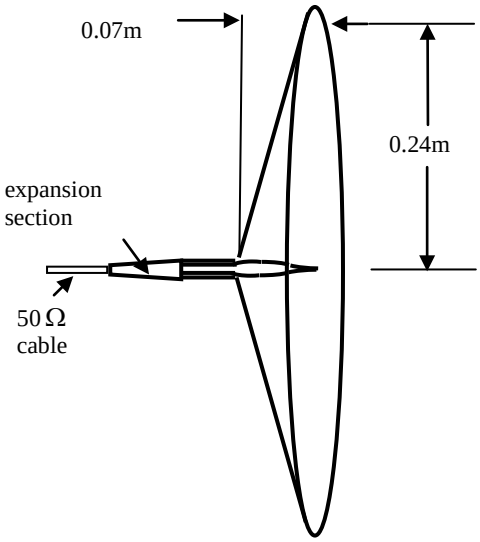

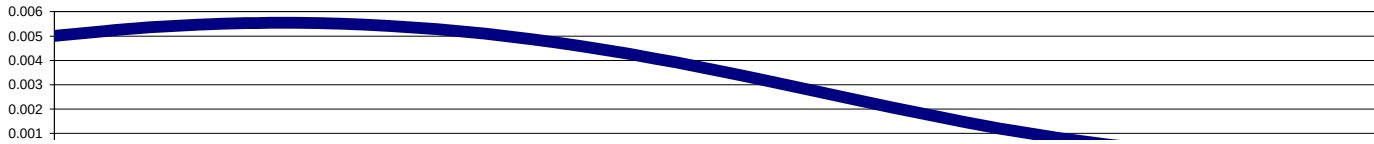

Figure 13. Profile of Central Electrode for the case of α = 3.429

This profile may be truncated for example at 4.5 cm where the impedance is $377\,\Omega$. It is not known but whether it is better to truncate than have the full length at a greater diameter than specified.

Choosing an exponential horn,

$$h(x/\ell) = \exp\left(\alpha\frac{x}{\ell}\right) \qquad g(x/\ell) = \left(\frac{b}{a}\right)^{-\left\{\left(1-\frac{x}{\ell}\right)^{-2}-1\right\}}\exp\left(\alpha\frac{x}{\ell}\right) \tag{57}$$

The central electrode profile is given in Figure 14.

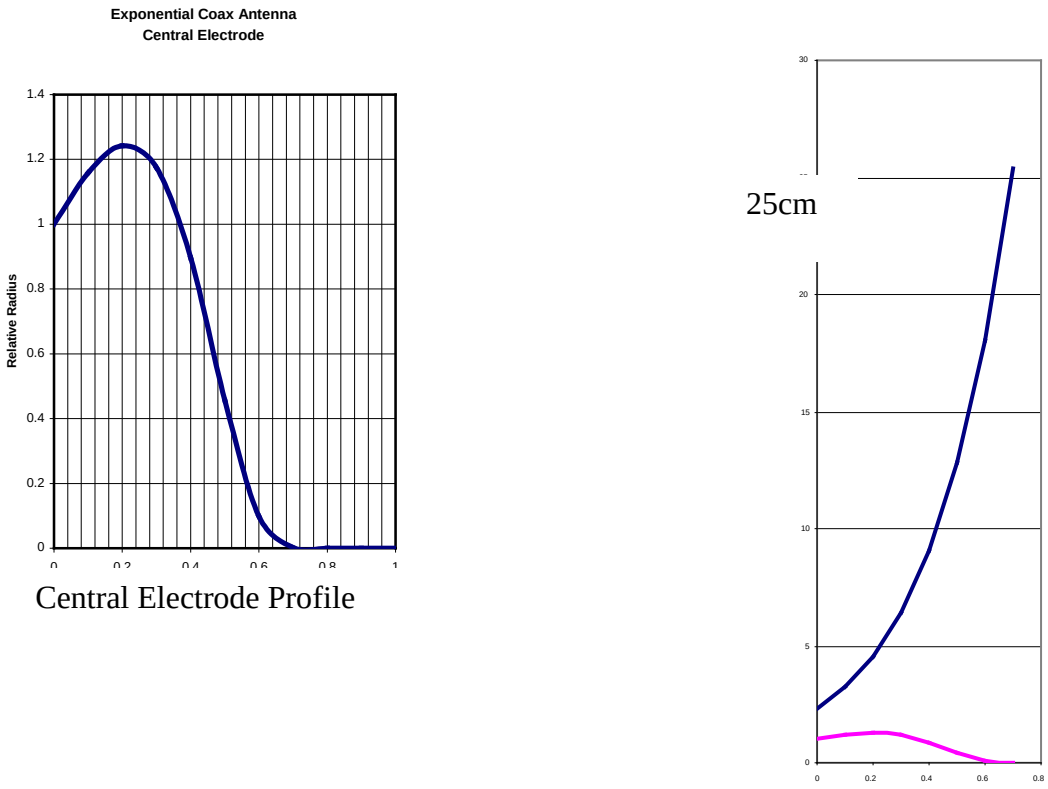

Figure 14. Electrode Profiles for $50\,\Omega$ /$377\,\Omega$ coaxial frequency independent antenna

6. The Vertical 'Monopole' Frequency Independent Antenna

The input impedance of a cone over a ground plane shown in Figure 15 is given by

$$Z = \frac{Z_0}{2\pi}\ln\left[\cot\left(\frac{\theta}{2}\right)\right] \tag{58}$$

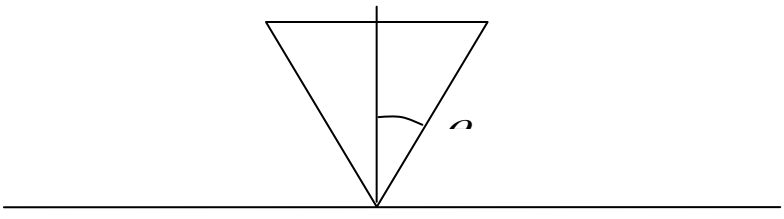

Figure 15. Mono-cone

To consider the variation of impedance with heig ht, the initial impedance is set at

$$Z(0) = \frac{Z_0}{2\pi} \ln\left[\cot\left(\frac{\theta_0}{2}\right)\right] \tag{59}$$

Expressing Z_0 in terms of the constants in equation (59) , substituting into equation (58) and imposing frequency independence

$$\frac{\ln\left[\cot\left(\frac{\theta}{2}\right)\right]}{\ln\left[\cot\left(\frac{\theta_0}{2}\right)\right]} = \left(1-\frac{h}{H}\right)^{-2} \tag{60}$$

Solving this for θ

$$\theta = 2\cot^{-1}\left\{\left[\cot\frac{\theta_0}{2}\right]^{\left(1-\frac{h}{H}\right)^{-2}}\right\} \tag{61}$$

Setting

$$r = h\tan(\theta)$$

$$\frac{r}{H} = \frac{h}{H}\tan\left\{2\cot^{-1}\left[\cot\left(\frac{\theta_0}{2}\right)\right]^{\left(1-\frac{h}{H}\right)^{-2}}\right\} \tag{62}$$

The profile of a 50 Ohm frequency independent monopole antenna is shown in Figure 16.

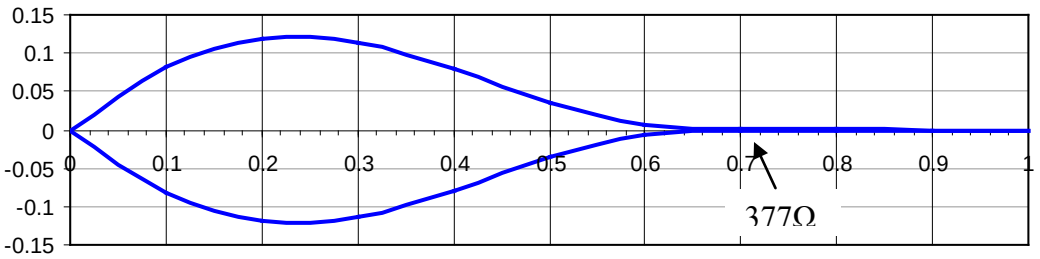

Figure 16. Profile of the 50Ω frequency independent monopole antenna

The antenna can again be truncated at h/H =0.636 corresponding to 377Ω for example. This is a limiting case of the co-axial antenna, with the difference that the feed is not part of the design.

Again in the case of a monocone antenna, using the Wu-King resistive loading profile several large antennas have been built for Nuclear Electromagnetic pulse (NEMP) simulation [19-20]. One of the largest such structure is the EMPRESS II HEMP simulator shown in Figure 17 [23]. EMPRES II (which is about 40m in height) uses a Wu-King resistive profile described in [18] to avoid reflections from the end of the monocone.

The shaping of the monocone can be an alternate method to continuously loading the monocone. It is anticipated in this case, the continuous loading to eliminate all reflections from the end of the monocone is superior to shaping the cone to achieve 377 Ohm impedance at the end of the cone.

Figure 17. EMPRESS II HEMP Simulator [reproduced from 24], which is basically a resistively loaded monocone antenna above a ground plane

7. References

[1] D. V. Giri and F. M. Tesche, "Energy Patterns of the Prototype Impulse Radiating Antenna (IRA),' Sensor and Simulation Note 550, 25 February 2010. This reference can be downloaded from www.ece.unm/summa/notes

[2] V. Rumsey, "Frequency Independent Antennas," IRE International Convention Record, volume 5, pp 114-118, 21-25 March 1966.

[3] C. E. Baum, Radiation of Impulse-Like Waveforms," Sensor and Simulation Note 321, 25 November 1989. This reference can be downloaded from www.ece.unm/summa/notes

[4] D. V. Giri et al., "Design, Fabrication and Testing of a Paraboloidal Reflector Antenna and Pulser System for Impulse-Like Waveforms," Invited Paper , IEEE Transactions on Plasma Science, Volume 25, Number 2, pp 318-326, April 1997.

[5] D. V. Giri, **High-Power Electromagnetic Radiators, Nonlethal Weapons and Other Applications**, published by Harvard University press, 2004.

[6] D. W. Fry, F. K. Goward, **Aerials for Centimetre Wavelengths**, Cambridge University Press, United Kingdom,1950

[7] S. Silver, **Microwave Antenna Theory and Design**, Radiation Laboratory Series, 1949.

[8] E Hallen, **Electromagnetic Theory**, Chapman & Hall, 1st U.S. Edition, December 1962

[9] H. B. Palmer, "Capacitance of a parallel-plate capacitor by the Schwartz-Christoffel transformation," Trans. AIEE, Vol. 56, pp. 363, March 1927.

[10] V. Leus, D. Elata, Fringing Field effect in electrostatic actuators Technion, Haifa, Israel, Technical Report ETR-2004-2, May 2004, available at: http://meeng.technion.ac.il/Research/TReports/2004/ETR-2004-02.pdf

[11] H. Yang, "Microgyroscope and Microdynamics," Ph. D. Dissertation, December, 2000.

[12] F. C. Yang and K. S. H. Lee, "Impedance of a two-conical-plate transmission line," Sensor and Simulation Note 221, November 1976. This reference can be downloaded from www.ece.unm/summa/notes

[13] C. E. Baum, "Low-frequency compensated TEM horn," Sensor and Simulation Note 377, 28 January 1992. This reference can be downloaded from www.ece.unm/summa/notes

[14] M. H. Vogel, "Design of the low-frequency compensation of an extreme-bandwidth TEM horn and lens IRA," Sensor and Simulation Note 391, 19 April 1996. This reference can be downloaded from www.ece.unm/summa/notes

[15] D. V. Giri, H. Lackner, G. Franceschetti, J. Tatoian V. Carboni and J. Lehr, "Design, Frabrication and Testing of a Timed Array of TEM Hrray for Beam Steering", Sensor and Simulation Note 469, 1 May 2002. This reference can be downloaded from www.ece.unm/summa/notes

[16] Y. Wang, Y. Chen and Q. Wang, "Application of a TEM horn antenna in radiating NEMP Simulator, 7th International Conference on Applied Electrostatics (ICAES-2012), Journal of Physics Conference Series 418 (2013), avaialble at www.iopscience.iop.org

[17] K. Shlager, G. S. Smith and J. G. Maloney, "Accurate Analysis of TEM Horn Antennas for Pulse Radiation," IEEE Transactions on Electromagnetic Compatibility, volume 38, Number 3, August 1996.

[18] T. T. Wu and R. W. P. King, "A cylindrical antenna with non-reflecting resistive loading," IEEE Transactions on Antennas and Propagation, Volume AP-13, pp 369-373, May 1965.

[19] C. E. Baum, Resistively loaded Radiating Dipole Based on a Transmission-Line Model, Sensor and Simulation Note 81, 7 April 1969. This reference can be downloaded from www.ece.unm/summa/notes

[20] D. V. Giri, "Time-Domain Radiated Fields of Resistively Loaded Biconical Antenna Based on a Transmission-Line Model, Sensor and Simulation Note 366, 1 April 1994. This reference can be downloaded from www.ece.unm/summa/notes

[21] D. V. Giri, "Impedance Matrix Characterization of an Incremental Length of a Periodic Array of Wave Launchers", Sensor and Simulation Note 316, 1 April 1989. This reference can be downloaded from www.ece.unm/summa/notes

[22] C. E. Baum, "Canonical Examples for High-Frequency Propagation on Unit Cell of Wave-0Launcher Array", Sesnsor and Simulation Note 317, 19 April 1989. This reference can be downloaded from www.ece.unm/summa/notes

[23] D. V. Giri, "A Family of Canonical Examples for High-Frequncy Propagation on Unit Cell of Wave-Launcher Array," Sensor and Simulaiton Note 318, 5 June 1989. This reference can be downloaded from www.ece.unm/summa/notes

[24] International ElectroTechncial Commission , "Testing and Measuremnt Techniques- High Altitude Electronagnetic Pulse (HEMP) Simulator Compendium", IEC 61000-4-32, 2002.